Springer

Available online at https://link.springer.com/journal/42241
http://www.jhydrodynamics.com
Journal of Hydrodynamics, 2022, 34(2): 286-298
https://doi.org/10.1007/s42241-022-0023-6

A general two-phase mixture model for sediment-laden flow in open channel

Jia-xing Li, Xin Chen*
Beijing Engineering Research Center of Safety and Energy Saving Technology for Water Supply Network System, China Agricultural University, Beijing 100083, China

(Received September 14, 2021, Revised October 22, 2021, Accepted October 29, 2021, Published online April 19, 2022)

Abstract: This work extends the sediment-laden mixture model with consideration of the turbulence damping and particle wake effects under the framework of improved efficiency and accuracy. The mixture model consists of the continuity and momentum equations for the sediment-laden mixture, and the continuity equation for the sediment. A theoretical formula is derived for the relative velocity between the water and sediment phases, with consideration of the effects of the pressure gradient, the shear stress and the lift force. A modified expression of the particle wake effect, inducing the local turbulence enhancement around the sediment particle, is employed to improve the turbulent diffusion of the coarse sediment. The k_m-ε_m model is proposed to close the mixture turbulence, with the turbulence damping effect due to the high sediment concentration expressed by the density-stratification term without an empirical parameter. The k_m-ε_m turbulence model requires smaller computational work and offers better results than an empirical density-stratification turbulence model in high sediment concentration cases. Consequently, with the proposed mixture model, the sediment transport in the open channel under a wide range of sediment sizes and concentrations can be revealed with the results in good agreement with experimental data for the velocity, the sediment concentration and the turbulent kinetic energy.

Key words: Sediment-laden flow, two-phase mixture model, particle wake effect, turbulence damping effect, density stratification

Introduction

The sediment transport is an issue constantly concerned in the studies of the river and costal engineering for a long while. In early studies, diffusion models were widely used for the vertical distribution of the sediment in the open channel and the classical power or exponential concentration formulas were obtained, such as the Rouse formula. In these concentration formulas, the sediment-laden interaction was neglected and the sediment was assumed to respond fully to the turbulent fluctuation of the velocity and, therefore, in cases of high sediment concentration or large inertia particle, their use is limited[1-2]. The diffusion models embodied by concentration formulas usually involve different sediment diffusion coefficients, and several improvements of the sediment diffusion coefficients were introduced by considering the diffusion enhancement of the coarse sediment and the turbulence damping due to the high sediment concentration[1-3].

In recent decades, the two-phase flow models have become popular and they are effective in the study of the sediment transport. The two-fluid (Euler-Euler) model is one of the two-phase flow models widely applied in the studies of the sediment transport. In the two-fluid model, the water and the sediment are treated as continuous phases in their motion and the sediment-laden interaction and the sediment friction and collision are considered for the massive particle flow[4-5]. Generally, the two-fluid model describes the sediment-laden flow better than the diffusion models except in the very dilute case where the particle stress becomes questionable and the continuous assumption of the particle phase fails[4]. However, a significant number of coupled equations are involved and they are hard to solve in the two-fluid models. Due to the large computational requirement, it is difficult to apply the two-fluid models to 3-D problems in engineering. Many simplifications were suggested for improving the efficiency of the two-fluid models. The mixture model based on

Project supported by the National Natural Science Foundation of China (Grant Nos. 41961144014, 51836010), the Chinese Universities Scientific Fund (Grant No. 2019TC133).
Biography: Jia-xing Li (1995-), Male, Ph. D. Candidate,
E-mail: ljxcau@cau.edu.cn
Corresponding author: Xin Chen,
E-mail: chenx@cau.edu.cn

the two-fluid model was proposed as a balance of the computational efficiency and accuracy[6-7]. In the mixture model, the water and the sediment are treated as a mixture phase and the continuity and momentum equations are applied for the mixture and a continuity equation is applied for the sediment. Instead of solving the partial differential momentum equation for the sediment, an algebraic expression for the relative velocity between the two phases, with consideration of the effects of the pressure gradient, the shear stress and the lift force, is employed to save the computational time[7]. Besides, with the mixture model, the errors originated from the phases coupling can be eliminated by approximately formulating the complicated inter-phase forces[6].

In the continuity equation for the sediment, the sediment diffusion coefficient plays a significant role in predicting the sediment distribution. In several researches, the sediment diffusion coefficient takes a value larger than that of the eddy viscosity and is positively related to w_{s0}/u_*, where u_* is the shear velocity and w_{s0} is the sediment falling velocity[1]. This relation is empirical and effective in a limited range. A wake region is found to exist behind a sediment particle due to the relative velocity between the water and the sediment particle, which enhances the turbulence intensity around the sediment particle[8] and in turns, the turbulent diffusion of the sediment[2]. Shi and Yu[2] proposed a theoretical description of the turbulence enhancement caused by the particle wake and demonstrated that the diffusion coefficient of the coarse sediment was larger than that of a fine one. Liang et al.[6] adopted the description of Shi and Yu[2] to improve the turbulent diffusion of the sediment in the mixture model, and have improved the prediction of the coarse sediment transport. However, in the case of the fine sediment, which follows the water very well, with the description of the turbulence enhancement caused by the particle wake, the turbulent diffusion of the sediment might be overestimated.

The turbulence in a two-phase flow is much more complicated than that in a single-phase flow because of the interaction between the two phases. Many experiments showed the damping effect due to the presence of the high concentration sediment on the turbulence intensity, the eddy viscosity and the sediment diffusion coefficient[9-10]. The turbulence damping effect is enhanced and the velocity profile is gradually changed with the increase of the sediment concentration[11]. The velocity change used to be attributed to the decrease of the Karman constant and the decrease of the eddy viscosity. A function of the local sediment concentration was developed to describe the turbulence damping effect by modifying the mixture eddy viscosity[1]. The function is fitted by several sets of experiment data and is accurate in a limited range. The turbulence damping effect was then attributed to the density stratification related to the sediment concentration gradient and a buoyancy term was introduced to represent the density stratification effect in the turbulent kinetic energy equation[12].

The two-equation closure is widely applied for the two-fluid model. The turbulence of the fluid phase is modeled by the k-ε model or the k-ω model, while the turbulence of the sediment phase is modeled by algebraic formulas[5, 13-14] or a turbulent kinetic energy equation[4]. In the original two-equation model, the turbulence damping effect is not considered for the sediment-laden flow of the high-concentration sediment[4]. The buoyancy terms accounting for the density stratification are empirically introduced in the k-ε model, to improve the performance of the k-ε model in case of high concentration sediment[13]. However, there is an uncertainty in the ε equation because the buoyancy term is associated with an empirical parameter related to the stratification state[12]. The k_m-ε_m model, only describing the turbulence of the mixture, is derived by a combination of the k equations and the ε equations of the fluid and of the sediment without the extra computation for the sediment turbulence. Since the density stratification term, accounting for the turbulence damping, is included, the k_m-ε_m model performs well in the study of the sediment transport and the open-channel flow under both the low- and high-concentration conditions[15].

This study aims to improve the sediment-laden mixture model with consideration of the turbulence damping effect and the particle wake effect under the framework of Liang et al.[6-7]. In this model, the local enhancement effects of the particle wake for both the fine and coarse sediments on the sediment turbulent diffusion are considered. The k_m-ε_m model, including the turbulence damping effect, is adopted to close the mixture turbulence.

1. Numerical model

1.1 *Governing equations*

The mixture model improves the computational efficiency and preserves the accuracy of a two-fluid model with the well-established relative velocity[7]. The present work follows Liang et al.'s[6] mass-weighted average and Reynolds average and the continuity and momentum equations of the mixture are:

$$\frac{\partial \rho_m}{\partial t}+\frac{\partial \rho_m u_{m,j}}{\partial x_j}=0 \tag{1}$$

$$\frac{\partial \rho_m u_{m,i}}{\partial t}+\frac{\partial \rho_m u_{m,i} u_{m,j}}{\partial x_j}=\rho_m g_i+\frac{\partial}{\partial x_j}(\sigma_{m,ij}+R_{m,ij}+\Omega_{m,ij}) \tag{2}$$

where ρ_m is the mixture density, u_m is the mixture velocity, the indices $i, j = 1,2,3$ are used for the components of a tensor and follow the Einstein summation convention, g is the body force, σ_m is the viscous stress of the mixture, R_m is the Reynolds stress of the mixture and Ω_m is the additional stress tensor resulting from the momentum exchange of the relative velocity[6].

The continuity equation for the sediment is

$$\frac{\partial \alpha_s}{\partial t}+\frac{\partial \alpha_s u_{m,j}}{\partial x_j}=\frac{\partial}{\partial x_j}\left(\frac{\alpha_s \alpha_f \rho_f}{\rho_m} w_j\right)+\frac{\partial}{\partial x_j}\left(\kappa_m \frac{\rho_f}{\rho_m}\frac{\partial \alpha_s}{\partial x_j}\right) \tag{3}$$

where α_f and α_s are the volumetric concentrations of the fluid and the sediment, ρ_f is the density of the fluid, w is the Reynolds-averaged relative velocity between the two phases and κ_m is the sediment diffusion coefficient given by $\kappa_m = \beta \nu_{mt}$, β is the reciprocal of the Schmidt number, ν_{mt} is the eddy viscosity of mixture. w is fixed by the theoretical formula proposed by Liang et al.[7]

$$w_i = \tau_s \frac{\alpha_f \rho_f}{\rho_m}(P_i + S_i + L_i) \tag{4}$$

where τ_s is the particle relaxation time scale, P_i, S_i and L_i, respectively, represent the pressure gradient effect, the shear stress effect and the lift force effect. Eq. (4) is derived from the momentum equations of a two-fluid model and is of similar accuracy with the two-fluid model[7] P_i and S_i are predominant in the horizontal and vertical directions, while L_i is considerable in the horizontal direction and is obtained by a predictor-corrector method[7]

Shi[16] proposed a theoretical expression of β for the turbulent diffusion enhancement caused by the particle wake:

$$\beta = 1.0 + 2.8 C_D^{4/3} \psi^{1/3} \frac{w_{s0}^2}{k_m} \tag{5}$$

$$\psi = 1.0 - \exp(-0.005 Re_s) \tag{6}$$

where C_D is the drag force coefficient, Re_s is the particle Reynolds number and ψ denotes the ratio of the wake length to the sediment diameter, d_s. The results of Eq. (5) agree well with those of experiments in a relatively wide range of Re_s, especially for the coarse sediment. However, Eq. (6) would overestimate the turbulence enhancement when the sediment size is small, because the fine sediment follows the water well and there is almost no wake region around the particle, i.e., $\psi = 0$. According to Shi's[16] suggestion, $\psi = 0$ is adopted when $Re_s < 2.0$ in this study. Consequently, ψ is remodeled based on Bagchi and Balachandar[8], i.e.:

$$\psi = 1.0 - \exp[-0.007(Re_s - 2.0)], \quad Re_s \geq 2.0 \tag{7a}$$

$$\psi = 0, \quad Re_s < 2.0 \tag{7b}$$

Figure 1 compares the values of β, computed with Eqs. (6), (7a) and (7b) in many cases[9, 11, 17-21], where $\beta_{\text{best-fitted}}$ is the β obtained by fitting the experimental sediment concentration and β_{comp} is computed with Eq. (5) combined with Eq. (6) or Eqs. (7a), (7b). Figure 1 shows that the values of β_{comp} obtained with both Eq. (6) and Eqs. (7a), (7b) are in good agreement with those of $\beta_{\text{best-fitted}}$ when $Re_s \geq 5.0$. Whereas, β_{comp} obtained with Eqs. (7a), (7b) is closer to $\beta_{\text{best-fitted}}$ than that obtained with Eq. (6) when $Re_s < 5.0$. With Eqs. (7a), (7b) and (5) gives better results of β for the fine sediment and similar results for the coarse sediment, as compared with Eq. (6).

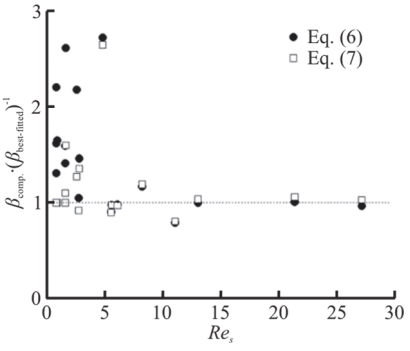

Fig. 1 Comparison of the value of β computed with Eqs. (6), (7a) and 7(b)

1.2 *Turbulence model*

The eddy viscosity, the turbulent kinetic energy (k_m) and its dissipation rate (ε_m) of the mixture are

defined as $\rho_m \nu_{mt} = \rho_f \nu_{ft} + \rho_s \nu_{st}$, $\rho_m k_m = \rho_f k_f + \rho_s k_s$ and $\rho_m \varepsilon_m = \rho_f \varepsilon_f + \rho_s \varepsilon_s$, where ρ_s is the density of sediment, ν_{ft}, k_f and ε_f, are the eddy viscosity, the turbulent kinetic energy and its dissipation rate of the fluid phase, respectively and ν_{st}, k_s and ε_s are those of the sediment. The k_m equation is obtained by the mass-weighted summation of k_f, k_s equations, as suggested by Lee et al.[14], and it gives satisfactory results for a wide range of sediment sizes and concentrations. Similarly, the ε_f equation is a concentration-weighted summation of ε_f, ε_s equations, as suggested by Lee et al.[14], where the ε_s equation is obtained by following the establishment of ε_f equation. The final k_m, ε_m equations are:

$$\frac{\partial \rho_m k_m}{\partial t} + \frac{\partial \rho_m k_m u_{m,j}}{\partial x_j} = \frac{\partial}{\partial x_j}\left(\rho_m \frac{\nu_{mt}}{\delta_k}\frac{\partial k_m}{\partial x_j}\right) + \rho_m (P_m - \varepsilon_m) + G_m \tag{8}$$

$$\frac{\partial \rho_m \varepsilon_m}{\partial t} + \frac{\partial \rho_m \varepsilon_m u_{m,j}}{\partial x_j} = \frac{\partial}{\partial x_j}\left(\mu_m + \rho_m \frac{\nu_{mt}}{\delta_\varepsilon}\frac{\partial \varepsilon_m}{\partial x_j}\right) + \frac{\varepsilon_m}{k_m}(C_{1\varepsilon}\rho_m P_m - C_{2\varepsilon}\rho_m \varepsilon_m + C_{3\varepsilon} G_m) \tag{9}$$

with

$$P_m = \left[-\frac{2}{3}k_m \delta_{ij} + \nu_{mt}\left(\frac{\partial u_{m,i}}{\partial x_j} + \frac{\partial u_{m,j}}{\partial x_i}\right)\right]\frac{\partial u_{m,i}}{\partial x_j} \tag{10}$$

$$G_m = -\omega_j \frac{\rho_s}{\tau_s}\kappa_m \frac{\partial \alpha_s}{\partial x_j} + \frac{\alpha_s \rho_s}{\tau_s}\omega_j^2 \tag{11}$$

where P_m is the production term, G_m represents the turbulence production due to the relative velocity, δ_{ij} is the Kronecker delta, ω is the mass-averaged relative velocity between the two phases[6], and ν_{mt} is computed by

$$\nu_{mt} = C_\mu \frac{k_m^2}{\varepsilon_m} \tag{12}$$

The constants are $\delta_k = 1.00$, $\delta_\varepsilon = 1.33$, $C_{1\varepsilon} = 1.44$, $C_{2\varepsilon} = 1.92$, $C_{3\varepsilon} = 1.20$ and $C_\mu = 0.09$.

The turbulence damping effect is important in modeling the turbulence of the sediment-laden flow. The diffusion terms in Eqs. (8), (9) can be expanded as:

$$\frac{\partial}{\partial x_j}\left(\rho_m \frac{\nu_{mt}}{\delta_k}\frac{\partial k_m}{\partial x_j}\right) = \frac{\partial}{\partial x_j}\left(\rho_m \frac{\nu_{mt}}{\delta_k}\frac{\partial k_m}{\partial x_j}\right) + (\rho_s - \rho_f)\frac{\nu_{mt}}{\delta_k}\frac{\partial \alpha_s}{\partial x_j}\frac{\partial k_m}{\partial x_j} \tag{13}$$

$$\frac{\partial}{\partial x_j}\left(\rho_m \frac{\nu_{mt}}{\delta_\varepsilon}\frac{\partial \varepsilon_m}{\partial x_j}\right) = \frac{\partial}{\partial x_j}\left(\rho_m \frac{\nu_{mt}}{\delta_\varepsilon}\frac{\partial \varepsilon_m}{\partial x_j}\right) + (\rho_s - \rho_f)\frac{\nu_{mt}}{\delta_\varepsilon}\frac{\partial \alpha_s}{\partial x_j}\frac{\partial \varepsilon_m}{\partial x_j} \tag{14}$$

The second term in the R.H.S. of Eqs. (13) or (14) is the density-stratification term accounting for the turbulence damping effect in the k_m-ε_m model. With this term, the motion of the turbulent eddy and the diffusion of the turbulent kinetic energy are hindered, along with the damping of the turbulence intensity[15, 22]. The density-stratification term and the turbulence damping will be discussed in Section 4.

1.3 *Boundary and initial conditions*

The present mixture model is applied for the open channel flows of different sediment sizes and concentrations. As shown in Fig. 2, in the selected cases, the sediment-laden flow is in the sedimentary equilibrium, where the sediment concentration does not vary in the flow direction.

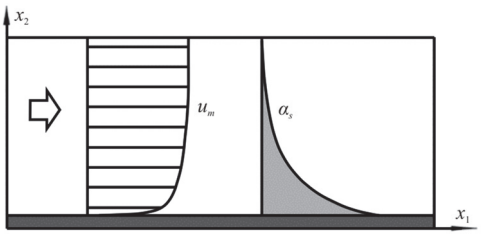

Fig. 2 Sketch of equilibrium sediment transport in open channel flow

At the inflow boundary, the horizontal velocity is given as the experimentally obtained flow rate, while other variables satisfy the condition of zero-gradient in the x_1-direction. All variables satisfy the zero-gradient condition at the outflow boundary. The velocity at the inflow boundary is adjusted by the outflow velocity during the computation.

At the top boundary, the rigid-lid assumption is employed. The vertical velocity of the mixture at the top boundary vanishes, and all other variables satisfy the zero-gradient condition in its normal direction except the sediment concentration, which satisfies the zero-flux condition[5, 23]

$$\kappa_m \frac{\partial \alpha_s}{\partial x_2} - u_{s,2}\alpha_s = 0 \tag{15}$$

where u_s is the velocity of sediment phase. Although the rigid-lid assumption is not perfectly justified near the free surface, its results do agree well with the experiment data in the open channel flow without a significant free surface effect[5, 14]. There are two methods to deal with the boundary condition of the turbulent kinetic energy (k_m) at the free surface, with two different distributions of the eddy viscosity. As one method, $k_m = 0$ is set at the free surface, causing a parabolic distribution of the eddy viscosity. As the other method, the condition of $\partial k_m / \partial x_2 = 0$ is applied at the free surface, causing a parabolic-constant distribution of the eddy viscosity[5]. The former method almost leads to the zero sediment concentration at the free surface, while the latter one leads to the non-zero sediment concentration at the free surface. The latter method is adopted in this study because a parabolic-constant distribution of the eddy viscosity is better than a parabolic one in the open-channel flow[14].

The sediment concentration affects the vertical velocity profile above the bed but the logarithmic velocity profile is still valid near the bed[14]. The wall function is adopted for the bottom boundary, i.e.:

$$\frac{u_{m,1}}{u_*} = \frac{1}{\kappa}\ln(Ey^*) \tag{16}$$

$$y^* = \frac{C_\mu^{1/4} k_m^{1/2} x_{2,P}}{\nu_{f0}} \tag{17}$$

$$\left.\frac{\partial k_m}{\partial x_2}\right|_{\text{wall}} = 0 \tag{18}$$

$$\varepsilon_m = \frac{C_\mu^{3/4} k_m^{3/2}}{\kappa x_{2,P}} \tag{19}$$

where $\kappa = 0.4$ is the Karman constant, E is a parameter related to the bed roughness and $E = 9.0$ for a smooth wall, $x_{2,P}$ is the height of the first grid adjacent to the bed and ν_{f0} is the kinematic viscosity of the fluid. k_m satisfies the condition of zero-gradient on the wall. Eq. (19) involves an assumption that the production of k_m is equal to its dissipation rate at the wall-adjacent grid based on the local equilibrium hypothesis. At the bottom boundary, the sediment concentration is set according to the experimental data. Because it is not the purpose of this paper to resolve the boundary layer structure of the sediment-laden flow, the bottom boundary condition is given at $x_2 = 0.02H$ outside the bed-load layer[6], where H is the flow depth.

1.4 *Numerical method*

The numerical model is established for both steady and unsteady flows, with the numerical method proposed by Chen et al.[5]. The governing equations are discretized over a staggered grid by the finite volume method, with the center-difference scheme used for the diffusion terms and the QUICK scheme used for the convection terms. The revised SIMPLE scheme is adopted for the coupled pressure-velocity. At each time step, the sediment concentration is computed first. Then, the velocities of the mixture are predicted and the pressure is corrected based on the solution of the pressure correction equation, derived from the overall mass conservation equation. The pressure and the velocities can therefore be updated to satisfy the mass and momentum conservations. Finally,

Table 1 Summary of the parameters for equilibrium transport validation[10-11]

Case	d_s /mm	w_{s0} /(10^{-2}m·s^{-1})	Re_s	u_* /(10^{-2}m·s^{-1})	H /10^{-2}m	U_m /(10^{-2}m·s^{-1})	$\alpha_{s,R}$	$\alpha_{s,m}$
C02	0.105	0.87	0.91	4.1	17.1	0.96	7.45×10^{-4}	2.11×10^{-4}
C20	0.105	0.87	0.91	4.1	17.0	0.96	1.71×10^{-2}	2.88×10^{-3}
C22	0.210	2.66	5.59	4.1	17.0	0.96	8.17×10^{-4}	1.79×10^{-4}
C31	0.210	2.66	5.59	4.1	17.2	0.96	9.06×10^{-3}	1.58×10^{-3}
C33	0.420	6.36	26.71	4.1	17.4	0.96	2.04×10^{-4}	4.09×10^{-5}
C40	0.420	6.36	26.71	4.5	17.1	0.96	1.79×10^{-3}	3.09×10^{-4}
SLF4	0.135	1.20	1.62	4.5	12.0	0.75	7.26×10^{-3}	4.19×10^{-4}
SAT	0.135	1.20	1.62	4.5	12.0	0.85	1.55×10^{-2}	1.48×10^{-3}

the turbulent kinetic energy and its dissipation rate and the relative velocity between the two phases can be readily computed. The time step always satisfies the CFL condition. The computation is terminated when the maximum relative error of the velocity between adjacent time steps is less than 10^{-6}. Additionally, the model is implemented in the vertical two-dimensions in this study.

2. Model validation in open channel flows

The parameters of the cases for the validation are shown in Table 1, where U_m is the mean velocity calculated by the flow rate, $\alpha_{s,R}$ is the sediment volume concentration at $0.05H$ and given by an interpolation of the experiment data and $\alpha_{s,m}$ is the depth-averaged sediment volumetric concentration. The sediment density in all cases is 2 650 kg/m^3. w_{s0} is given according to the experiment in the cases of SLF4, SAT[10] and Chang and Liou's formula[24] in other cases.

Coleman[11] performed three sets of experiments in a smooth channel of 15 m in length and 0.356 m in width, i.e., C01-C20, C21-C31 and C32-C40, with the grain sizes of 0.105 mm, 0.210 mm and 0.420 mm, respectively. The flow rate is 0.0064 m/s and thus the flow depth is around 0.17m. The sediment concentration is gradually increased from zero to a value under nearly saturated conditions in each set of experiments, where C02, C22 and C33 are the most dilute cases, and C20, C31 and C40 are the saturated cases. Similarly, Cellino and Graf[10] performed eight experiments in the open-channel, from the clear-water condition to the saturated condition, using the grain size of 0.135 mm with a rough bed, where SLF4 is the case with a medium sediment concentration and SAT is the saturated case with a sand layer of about 2 mm on the bed. The flow rate increases with the increase of the sediment concentration while the depth maintains constant of $H = 0.12$ m.

Figure 3 shows the comparison of the horizontal velocity of the mixture between the computed and experimental results, where "CX2011" is the two-phase model result of Chen et al.[5]. The computed variables (u_m, k_m, ν_{mt}) of the mixture are very close to those of the water phase because the sediment concentration is much smaller than that of the water phase. The relative error, $\left|\text{computation} / \text{experiment} - 1\right|$, is used to evaluate the accuracy of the computed velocity. The mean relative error is shown in Table 2. The computed results of the velocity are in good agreement with the experiments except the cases of Cellino and Graf[10]. The experimental flow rate is larger than the integration of the experimental velocity at the centerline of the test section in the Cellino and Graf's two cases[10], and thus the velocity according to the experimental flow rate is overestimated. The decrease of the velocity at the centerline is mainly caused by the wake flow near

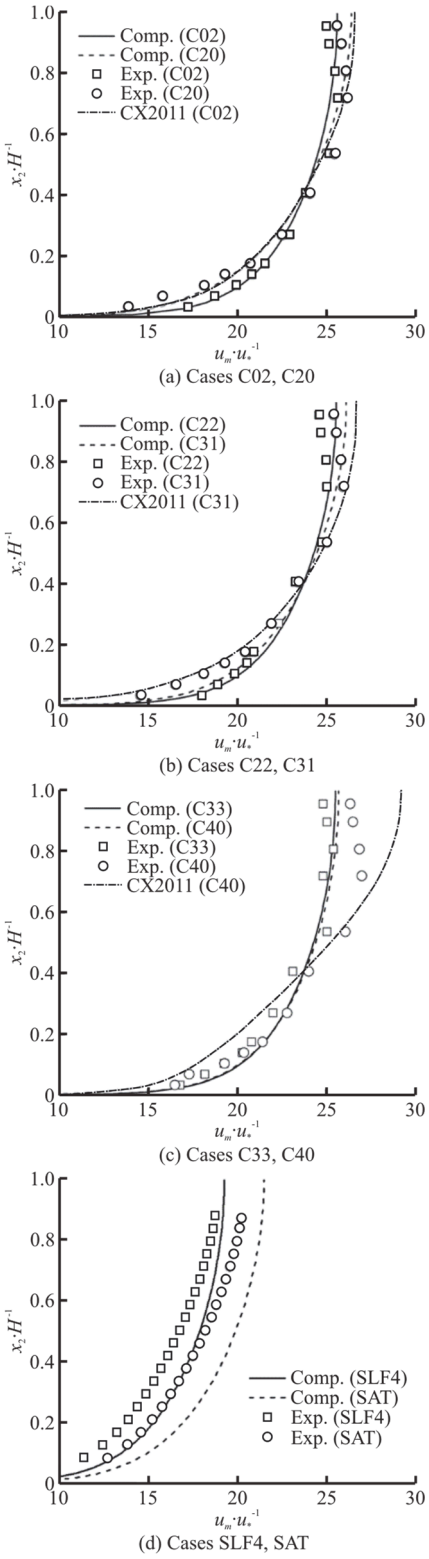

Fig. 3 Horizontal velocity profiles

the free surface and the secondary flow near the sidewall. The decrease is enhanced by the rough bed in Cellino and Graf's experiments[10], but is not significant in the smooth bed experiments of Coleman[11]. Both the computa- tions and the experiments show the effect of the sediment concentration on the velocity profile as indicated in Fig. 3. With the increase of the sediment concentration, the velocity and its gradient decrease in the near-bed region and increase in the upper region as a compensation. Chen et al.'s[5] two-fluid model also gives a similar variation of the velocity profile as obtained in Coleman's[11] experiments. Compared with Chen et al.'s two-fluid model, the present mixture model gives the results of similar accuracy but with fewer coupled equations. According to Liang et al.[6], the mixture model saves 80%-90% of the computational time in the equilibrium transport cases compared to the complete two-fluid model with a similar numerical scheme.

Table 2 Mean values of relative and logarithm errors for the present model

Case	Relative error of u_m /%	Logarithm error of α_s /%	
		Present model	Rouse formula
C02	1.34	1.87	0.89
C20	3.92 (3.67)	3.66 (11.42*)	12.13
C22	2.09	1.50	29.05
C31	4.50 (3.02)	3.89 (10.42*)	30.23
C33	3.01	1.62	85.38
C40	3.99 (6.48)	2.26 (8.56*)	100.28
SLF4	8.34	7.10	7.17
SAT	9.44	11.51	16.78

Note: *Data in bracket is the error of Chen et al.'s computation[5].

Figure 4 compares the computed and experimental sediment concentrations, as well as the results of the Rouse formula. Table 2 shows the logarithm error, $\left|\lg(\text{experiment})/\lg(\text{computation})-1\right|$, which is used to evaluate the accuracy of the computed sediment concentration. Intuitively, the present model in general enjoys a better accuracy than the Rouse formula, especially in some saturated cases (C20, SAT) and large sediment cases (C22, C31, C33 and C40). The Rouse formula is derived from the diffusion equation without the consideration of the enhancement effect of the particle wake and the damping effect of the density -stratification on the diffusion of the sediment, and it is only accurate in the case C02 where the sediment particles are of low inertia and the sediment concentration is very low. Therefore, the Rouse formula will produce significant deviations in large sediment or high concentration cases, as shown in Table 2. For the coarse sediment, the computation of the sediment concentration is improved with the

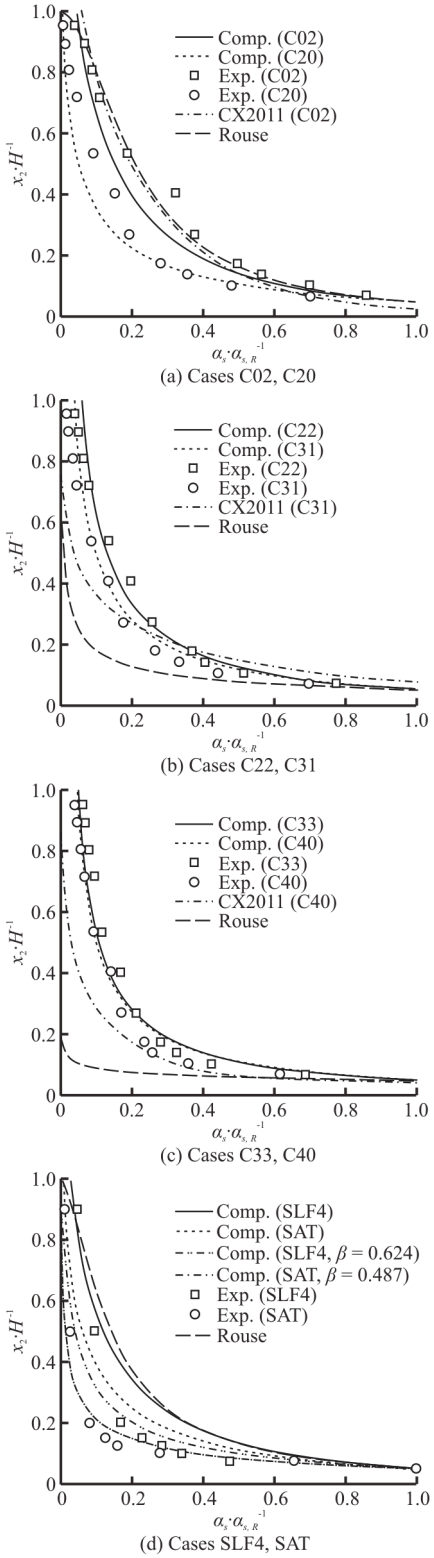

Fig. 4 Sediment concentration profiles

turbulence enhancement effect described by Eq. (5). The dimensionless sediment concentration decreases with the increase of the sediment concentration, as shown in Fig. 4, which is identified by the present

mixture model and many experiments[10-11]. The turbulence damping effect included in the k_m - ε_m model is responsible for the suppressed turbulent diffusion of the sediment in the saturated cases. Without the turbulence damping effect in the turbulence model and with the diffusion enhancement induced by the particle wake, the sediment concentration obtained by Chen et al.[5] is of lower accuracy than the present model. In the cases SLF4, SAT, the computed sediment concentration is larger than the experiments, as shown in Fig. 4(d), corresponding to an overestimated sediment diffusion coefficient. The overestimation can be improved by adopting the suggestion of taking a value $\beta < 1.0$ for the sediment-water flows over a movable sand bed without a bed form[25], and $\beta = 0.624,\ 0.487$ in the cases SLF4, SAT[10], respectively.

Figure 5 compares the computed k_m in the mixture in cases of different sediment concentrations. k_m decreases with the increase of the sediment concentration, and the turbulence damping becomes significant under high sediment concentration (gradient) conditions. Such damping effect is evident in many observations, such as Wang and Qian's[9] and Cellino and Graf's[10] natural sediment experiments in open channels, and Matinpour et al.'s[26] experiments in a mixing box. The turbulence damping is related to the gradient of the sediment concentration, as shown by Eq. (13) in the present model. In addition, the turbulence damping in the computation is observed near the top due to the top setting of k_m $(\partial k_m / \partial x^2 = 0)$, and the damping disappears if k_m at the top is set to be zero. In Fig. 5(d), the computation results generally agree with the experiments. Obvious difference of k_m is observed between the cases SLF4, SAT in the computations, as is consistent with the obvious difference of u_m in Fig. 3(d). In the experimental data of Fig. 5(d), the turbulence damping is significant at the near-bed region of high sediment concentration and it gradually decreases away from the bed. The turbulence damping in the computation data of Figs. 5(a), 5(d) is also significant, with a similar vertical trend as that of the experiments. The suspended sediment concentration is very low in the coarse sediment cases C32, C40. Therefore, the turbulence damping is insignificant in Fig. 5(c) and the difference of k_m between the two cases is small.

The variation of the velocity against the increased sediment concentration is characterized by the increase of the velocity gradient, and is attributed to the decrease of the eddy viscosity[1]. The experiments of Matinpour et al.[26] show that the turbulent kinetic energy and the eddy viscosity decrease with the increase of the sediment concentration. In the present k_m - ε_m model, the density-stratification term accounts for the turbulence damping, for the decrease of k_m and ν_{mt} as shown in Figs. 5, 6. The value of

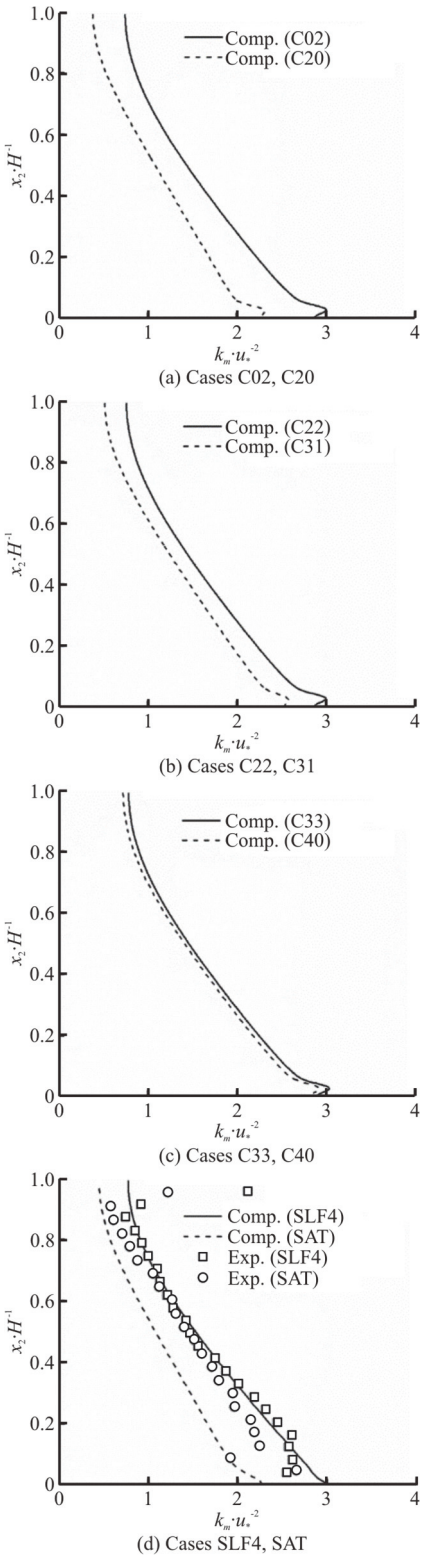

Fig. 5 Turbulent kinetic energy profiles

ν_{mt} in the saturated case is significantly smaller than that in the dilute case. The value of u_m is directly related to that of ν_{mt} in the open channel flows. The horizontal momentum equation in the steady open-hannel flow can be simplified as

$$\left(\nu_{mt}+\frac{\mu_m}{\rho_m}\right)\frac{\partial u_{m,1}}{\partial x_2}=u_*^2\left(1-\frac{x_2}{H}\right) \tag{20}$$

According to Eq. (20), the decrease of ν_{mt} leads to the increase of the velocity gradient, as shown in Fig. 3. With the standard wall function applied at the bottom boundary, a smaller value of $u_{m,1}$ is obtained at the first grid above the bed for the sediment-laden flow than that for the clear water flow, as is consistent with the velocity distribution near the bottom observed in the experiments[9, 11, 18]. Herrmann and Madsen[27] illustrated that the sediments near the bottom induce a drag effect on the water to enhance the effective flow resistance and to decrease the near-bed velocity. The drag effect becomes more significant as the sediment concentration increases. When the sediment concentration increases, the decrease of ν_{mt} due to the turbulence damping effect will reduce the sediment diffusion coefficient and thus the dimensionless sediment concentration as shown in Fig. 4, and as observed in many experiments[10, 11, 26].

3. Discussion for density-stratification term

As mentioned above, the turbulence damping induced by the density-stratification term is considered in the k_m-ε_m model. According to Eq. (8), the dimensionless k_m equation for the steady open-channel flow becomes

$$\underbrace{\frac{H}{u_*^3\rho_m}\frac{\partial}{\partial x_2}\left(\rho_m\frac{\nu_{mt}}{\delta_k}\frac{\partial k_m}{\partial x_2}\right)}_{\text{TD}}+\underbrace{\frac{H}{u_*^3\rho_m}\nu_{mt}\left(\frac{\partial u_{m,1}}{\partial x_2}\right)^2}_{\text{TP}}-$$

$$\underbrace{\frac{H}{u_*^3\rho_m}\varepsilon_m}_{\text{TE}}+\underbrace{\frac{H}{u_*^3\rho_m}\frac{\alpha_s\rho_s}{\tau_s}\omega_1^2}_{\text{TR}}=0 \tag{21}$$

where TD, TP, TE and TR denote the diffusion term, the production term, the dissipation term and the relative velocity term, respectively. The dilute Case C02 is compared with the saturated case C20 in Fig. 7 for TP, TE and TD. TR is not shown because its magnitude is extremely small in the open channel flow, with a very little effect on k_m [14]. TP, TE are in a relative equilibrium in the open channel flow. Therefore, TD is relatively small and only considerable near the bed. The distributions of TP, TE and TD in the two cases almost coincide with each other in Fig. 7. The differences of the two cases mainly appear near the bottom, where the difference of the velocity gradient is relatively large according to Fig. 3(a).

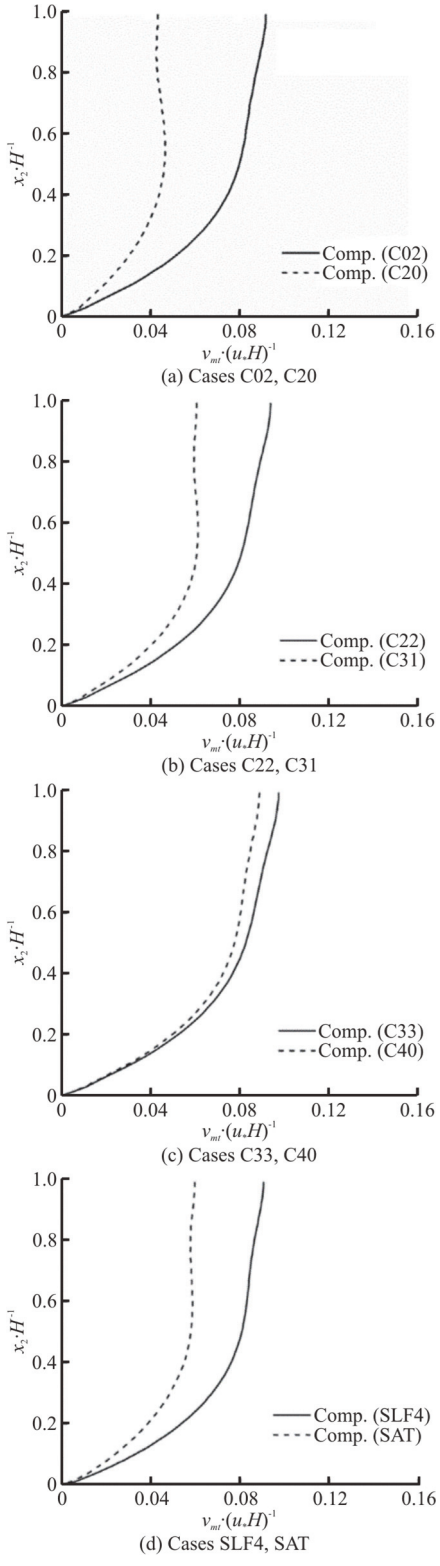

Fig. 6 Eddy viscosity profiles

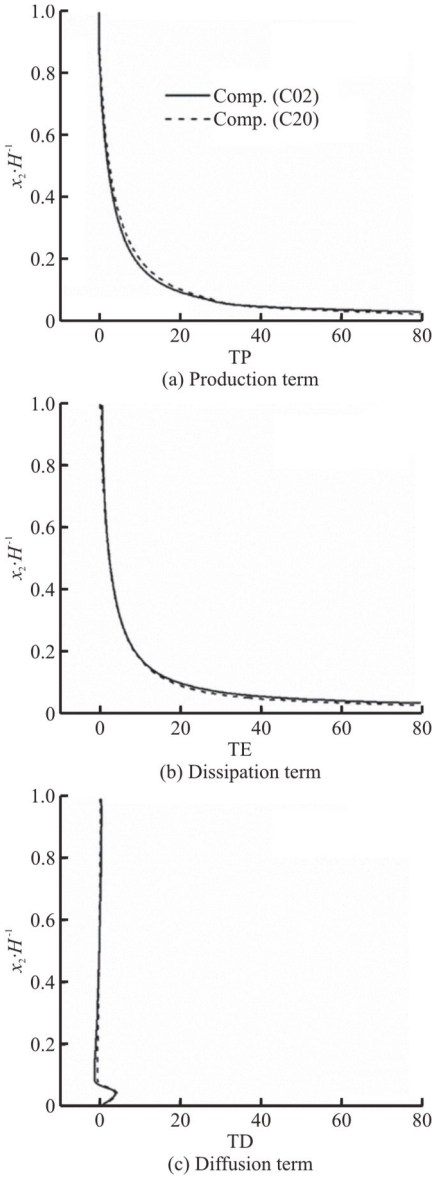

Fig. 7 Distributions of production term, dissipation term and diffusion term in cases C02, C20

Although the magnitude of TD is much smaller than those of TE, TP, the density-stratification term in the diffusion term (Eq. (13)) is important to the distributions of the velocity, the turbulence, the eddy viscosity and the concentration. The k_m-ε_m model can be reduced to:

$$\frac{\partial}{\partial x_2}\left(\frac{\nu_{mt}}{\delta_k}\frac{\partial k_m}{\partial x_2}\right)+\nu_{mt}\left(\frac{\partial u_{m,1}}{\partial x_2}\right)^2-\varepsilon_m+\frac{\alpha_s\rho_s}{\tau_s\rho_m}\omega_1^2=0 \quad (22)$$

$$\frac{\partial}{\partial x_2}\left(\frac{\nu_{mt}}{\delta_k}\frac{\partial \varepsilon_m}{\partial x_2}\right)+\frac{\varepsilon_m}{k_m}\left[C_{1\varepsilon}\nu_{mt}\left(\frac{\partial u_{m,1}}{\partial x_2}\right)^2-C_{2\varepsilon}\varepsilon_m+C_{3\varepsilon}\frac{\alpha_s\rho_s}{\tau_s\rho_m}\omega_1^2\right]=0 \quad (23)$$

which are hold in the steady open channel flow without consideration of the density-stratification term in Eqs. (13), (14).

Figure 8 compares the results of Eqs. (22), (23) with those of the k_m-ε_m model for the high-concentration Case C20. The results of the k-ε model for the clear water (CW) under the same flow condition are also plotted for comparison. Fig. 8 shows that the results of Eqs. (22), (23) in case C20 almost coincide with the results of the k-ε model for the clear water, and are obviously different from the results of the complete k_m-ε_m model. The k_m-ε_m model without the density-stratification term cannot reflect the turbulence damping effect on k_m, ε_m and ν_{mt}, and fails to predict the velocity profile under the high-concentration condition. The degradation confirms that the density-stratification term is mainly responsible for the differences between the saturated and dilute cases. In the early k_f-ε_f model, the turbulence damping effect is not considered for the dilute flow[4]. The modified k_f-ε_f model[6], with empirically introduced buoyancy term to account for the density stratification, is effective for the non-dilute sediment transport. Here, the present k_m-ε_m model is compared with the modified k_f-ε_f model, i.e.:

$$\frac{\partial \alpha_f\rho_f k_f}{\partial t}+\frac{\partial \alpha_f\rho_f k_f u_{f,j}}{\partial x_j}=\frac{\partial}{\partial x_j}\left(\rho_f\frac{\nu_{ft}}{\delta_k}\frac{\partial \alpha_f k_f}{\partial x_j}\right)+\alpha_f\rho_f(P_f-\varepsilon_f)+G_{f1}+G_{f2} \quad (24)$$

$$\frac{\partial \alpha_f\rho_f \varepsilon_f}{\partial t}+\frac{\partial \alpha_f\rho_f \varepsilon_f u_{f,j}}{\partial x_j}=\frac{\partial}{\partial x_j}\left(\rho_f\frac{\nu_{ft}}{\delta_\varepsilon}\frac{\partial \alpha_f \varepsilon_f}{\partial x_j}\right)+\frac{\varepsilon_f}{k_f}[\alpha_f\rho_f(C_{1\varepsilon}P_f-C_{2\varepsilon}\varepsilon_f)+C_{3\varepsilon}G_{f1}+C_{4\varepsilon}G_{f2}] \quad (25)$$

$$G_{f1}=-2\rho_s\alpha_s k_f(1-\lambda)\tau_s^{-1},\quad G_{f2}=(\rho_s-\rho_f)g\kappa_m\frac{\partial \alpha_s}{\partial x_i} \quad (26)$$

where G_{f1} represents the turbulent kinetic energy exchange between the water and the sediment, λ is the particle response factor, G_{f2} is the buoyancy term accounting for the turbulence damping caused by

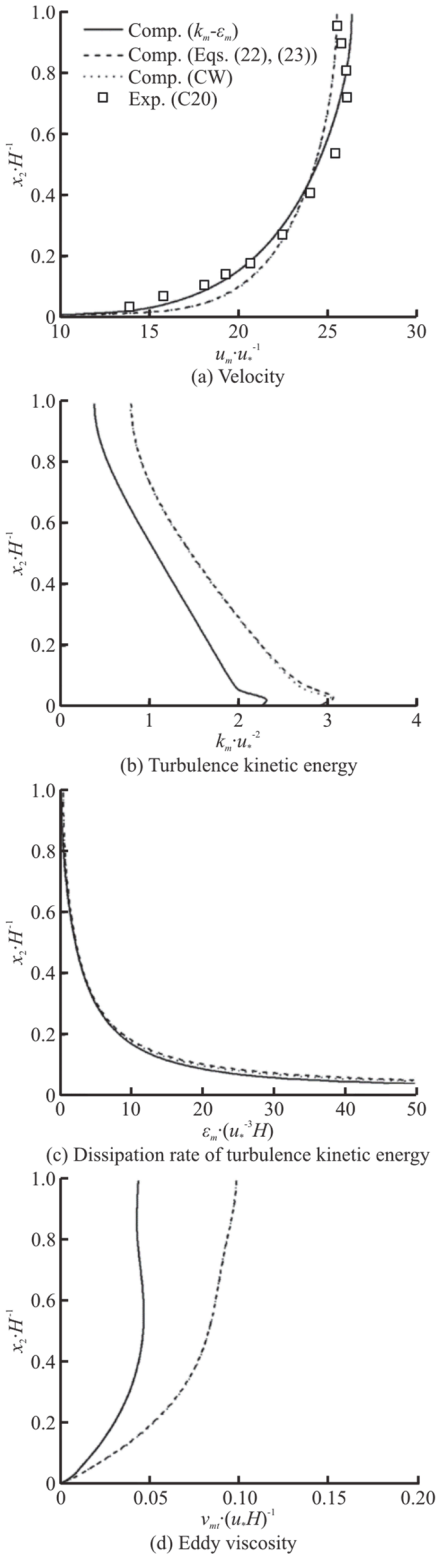

Fig. 8 Computations with and without density-stratification term

the density stratification effect, $C_{4\varepsilon}$ is associated with the buoyancy term and set to be 1.2[6]. The turbulent kinetic energy and the turbulent viscosity of the sediment, k_s, ν_{st}, are calculated from algebraic formulas[6]. In both the modified k_f-ε_f model and the k_m-ε_m model, the density-stratification effect is independent of the sediment diameters, as is consistent with the experiments of Graf and Cellino[25].

The computation based on the present k_m-ε_m model takes slightly less time than that of the modified k_f-ε_f model. Both models can well predict the velocity and the concentration in dilute cases. Figure 9 only compares the two turbulence models based on case C20. k_m, ν_{mt} are computed based on the definitions of Section 2.2 in the modified k_f-ε_f model. Some differences exist in the computations between the present k_m-ε_m model and the modified k_f-ε_f model. The buoyancy term is negative in the modified k_f-ε_f model, and its magnitude is almost equivalent to that of the dissipation term in case C20. Therefore, the computed results are very sensitive to the value of $C_{4\varepsilon}$. Figure 9 shows that the modified k_f-ε_f model with $C_{4\varepsilon}=1.2$ yields a similar value of k_m but a smaller value of ε_m and a larger value of ν_{mt} compared to the k_m-ε_m model, and the k_m-ε_m model makes better predictions of the velocity and the concentration than the modified k_f-ε_f model in case C20 and also in the high-concentration case SAT. Several researches suggested that $C_{4\varepsilon}=1.0$ for the unsteady stratified flow and $C_{4\varepsilon}=0$ for the steady stratified flow[12]. The modified k_f-ε_f model with $C_{4\varepsilon}=0$ would yield a larger value of ε_m than that with $C_{4\varepsilon}=1.2$ and provides the results almost the same as that provided by the k_m-ε_m model. Compared with the modified k_f-ε_f model, the k_m-ε_m model automatically includes the density-stratification effect and avoids the selection of $C_{4\varepsilon}$.

4. Conclusions

This work improves the mixture model[6] with consideration of the turbulence damping and the particle wake for the sediment transport in the open channel. The mixture model is developed from a framework, with a well-established relative velocity, a good computational speed and an improved accuracy. The formulas for the local turbulence enhancement of the particle wake are obtained covering both the fine

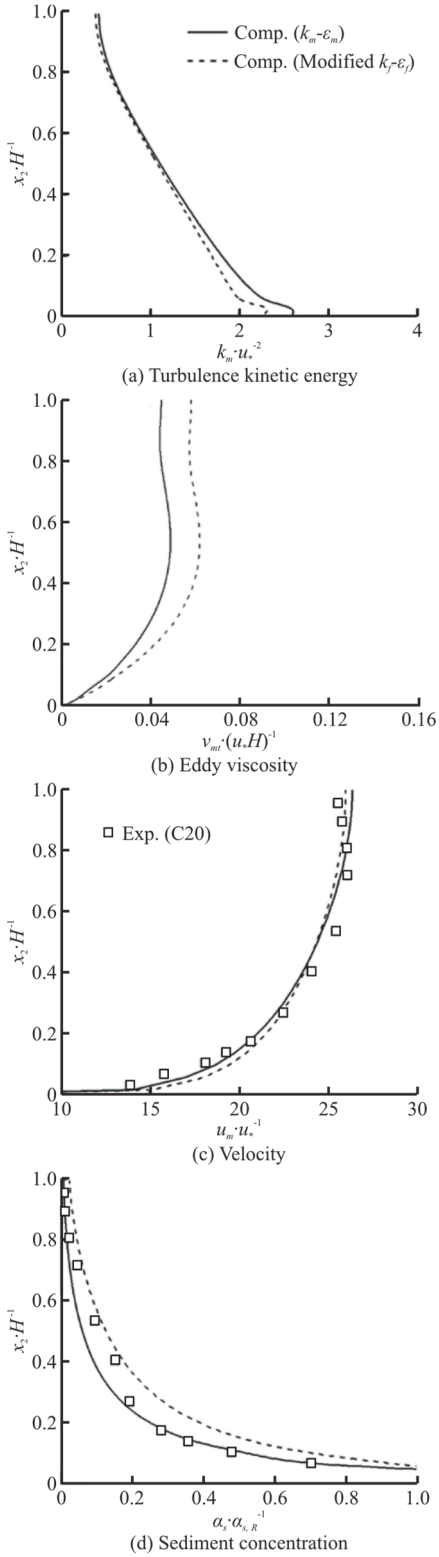

Fig. 9 Comparison between the present k_m - ε_m model and the modified k_f - ε_f model

and coarse sediment cases. The k_m - ε_m model obtained by the concentration-weighted summation of k_f - ε_f - k_s model[14] closes the mixture turbulence. The density-stratification terms accounting for the turbulence damping effect are included in the diffusion terms of the equations of k_m, ε_m.

The proposed mixture model is validated by the sediment transport data of the open channel flow covering a wide range of sediment sizes and concentrations. Concentration profiles of different sediment sizes are reasonably obtained with consideration of the local turbulence enhancement of the particle wake. With the mixture model, the differences between dilute and saturated sediment-laden flows are successfully identified, for the profiles of the velocity, the sediment concentration, the turbulent kinetic energy and the eddy viscosity. Generally, the turbulent kinetic energy and the eddy viscosity of the mixture decrease with the increase of the sediment concentration due to the turbulence damping effect. Therefore, the sediment diffusion coefficient and the dimensionless sediment concentration decrease with the increase of the sediment concentration. The mixture velocity and its gradient decrease near the channel bottom and increase near the channel top in compensation.

The decomposition of the proposed k_m equation shows a relative balance between the production and dissipation terms in the steady open channel flow. The diffusion term is relative small, with the density-stratification term and is considerable near the bed. When the density-stratification term is absent, the k_m - ε_m model is almost reduced to the k - ε model for the clear water, and the results in the saturated case are almost degraded to those in the clear-water case. The degradation further confirms that the differences between the saturated and dilute cases are caused by the density-stratification term. Compared to a modified k_f - ε_f model with a buoyancy term accounting for the density stratification, the k_m - ε_m model makes better predictions of the velocity and the concentration in the high sediment-concentration cases without depending on an empirical parameter associated with the density stratification.

References

[1] Li Y., Xie L., Su T. C. Profile of suspended sediment concentration in submerged vegetated shallow water flow [J]. *Water Resources Research*, 2020, 56(4): e2019WR025551.

[2] Shi H., Yu X. An effective Euler-Lagrange model for suspended sediment transport by open channel flows [J]. *International Journal of Sediment Research*, 2015, 30(4): 361-370.

[3] Huai W., Yang L., Wang W. Predicting the vertical low suspended sediment concentration in vegetated flow using a random displacement model [J]. *Journal of Hydrology*,

2019, 578: 124101.
[4] Hsu T. J., Jenkins J. T., Liu P. L. F. On two-phase sediment transport: Sheet flow of massive particles [J]. *Proceedings of the Royal Society A: Mathematical, Physical and Engineering Sciences*, 2004, 460(2048): 2223-2250.
[5] Chen X., Li Y., Niu X. et al. A general two-phase turbulent flow model applied to the study of sediment transport in open channels [J]. *International Journal of Multiphase Flow*, 2011, 37(9): 1099-1108.
[6] Liang L., Yu X., Bombardelli F. A general mixture model for sediment laden flows [J]. *Advances in Water Resources*, 2017, 107: 108-125.
[7] Liang L., Yu X., Bombardelli F. A general formulation of relative motion between two phases in sediment-laden water flows [J]. *International Journal of Multiphase Flow*, 2018, 109: 63-83.
[8] Bagchi P., Balachandar S. Response of the wake of an isolated particle to an isotropic turbulent flow [J]. *Journal of Fluid Mechanics*, 2004, 518: 95-124.
[9] Wang X., Qian N. Turbulence characteristics of Sediment-laden flow [J]. *Journal of Hydraulic Engineering, ASCE*, 1989, 115(6): 781-800.
[10] Cellino M., Graf W. H. Sediment-laden flow in open channels under noncapacity and capacity conditions [J]. *Journal of Hydraulic Engineering, ASCE*, 1999, 125(5): 456-462.
[11] Coleman N. L. Effects of suspended sediment on the open-channel velocity distribution [J]. *Water Resources Research*, 1986, 22(10): 1377-1384.
[12] Winterwerp J. C. Stratification effects by cohesive and noncohesive sediment [J]. *Journal of Geophysical Research: Oceans*, 2001, 106(C10): 22559-22574.
[13] Jha S. K., Bombardelli F. Toward two-phase flow modeling of nondilute sediment transport in open channels [J]. *Journal of Geophysical Research: Earth Surface*, 2010, 115(F3): F001347.
[14] Lee C. H., Huang Z., Chiew Y. M. A multi-scale turbulent dispersion model for dilute flows with suspended sediment [J]. *Advances in Water Resources*, 2015, 79: 18-34.
[15] Huang H., Zhan H., Zhong D. et al. Turbulent mechanisms in open channel sediment-laden flows [J]. *International Journal of Sediment Research*, 2019, 34(6): 550-563.
[16] Shi H. Two-phase flow models and their applications to sediment transport [D]. Doctoral Thesis, Beijing, China: Tsinghua University, 2016(in Chinese).
[17] Kundu S., Ghoshal K. Effects of non-locality on unsteady nonequilibrium sediment transport in turbulent flows: A study using space fractional ADE with fractional divergence [J]. *Applied Mathematical Modelling*, 2021, 96: 617-644.
[18] Eggenhuisen J. T., Tilston M. C., de Leeuw J. et al. Turbulent diffusion modelling of sediment in turbidity currents: An experimental validation of the Rouse approach [J]. *The Depositional Record*, 2020, 6: 203-216.
[19] Nezu I., Azuma R. Turbulence characteristics and interaction between particles and fluid in particle-laden open channel flows [J]. *Journal of Hydraulic Engineering, ASCE*, 2004, 130(10): 988-1001.
[20] Zhang B., Wu B., Li S. et al. Large eddy simulation of sediment transport in high flow intensity by discrete particle method [J]. *Journal of Hydraulic Research*, 2020, 59(4): 605-620.
[21] Muste M., Yu K., Fujita I. et al. Two-phase versus mixed-flow perspective on suspended sediment transport in turbulent channel flows [J]. *Water Resources Research*, 2005, 411(10): 312-321.
[22] Salimi-Tarazouj A., Hsu T. J., Traykovski P. et al. A numerical study of onshore ripple migration using a Eulerian two-phase model [J]. *Journal of Geophysical Research: Oceans*, 2021, 126(2): e2020JC016773.
[23] Li Z. W., Huai W. X., Han J. Large eddy simulation of the interaction between wall jet and offset jet [J]. *Journal of Hydrodynamics*, 2011, 23(5): 544-553.
[24] Chang H. K., Liou J. C. Discussion on a fall-velocity equation by Nian-Sheng Cheng [J]. *Journal of Waterway Port Coastal and Ocean Engineering*, 2001, 127(4): 250-251.
[25] Graf W. H., Cellino M. Suspension flows in open channels, experimental study [J]. *Journal of Hydraulic Research*, 2002, 40(4): 435-447.
[26] Matinpour H., Bennett S., Atkinson J. et al. Modulation of time-mean and turbulent flow by suspended sediment [J]. *Physical Review Fluids*, 2019, 4(7): 074605.
[27] Herrmann M. J., Madsen O. S. Effect of stratification due to suspended sand on velocity and concentration distribution in unidirectional flows [J]. *Journal of Geophysical Research: Oceans*, 2007, 112(2): C02006.